Available online at www.sciencedirect.com
ScienceDirect
Molecular Phylogenetics and Evolution 44 (2007) 1–14
MOLECULAR PHYLOGENETICS AND EVOLUTION
www.elsevier.com/locate/ympev

Calibration of a molecular clock in tits (Paridae)—Do nucleotide substitution rates of mitochondrial genes deviate from the 2% rule?

Martin Päckert [a,*], Jochen Martens [b], Dieter Thomas Tietze [b], Christian Dietzen [c], Michael Wink [c], Laura Kvist [d]

[a] *Staatliche Naturhistorische Sammlungen, Museum für Tierkunde, Königsbrücker Landstraße 159, 01109 Dresden, Sachsen, Germany*
[b] *Institut für Zoologie, Saarstraße 21, 55099 Mainz, Germany*
[c] *Institut für Pharmazie und Molekulare Biotechnologie, Im Neuenheimer Feld 364, 69120 Heidelberg, Germany*
[d] *Department of Biology, University of Oulu, Linnanmaa, 90014 Oulu, Finland*

Received 11 April 2006; revised 18 December 2006; accepted 5 March 2007
Available online 19 March 2007

Abstract

The ongoing debate on the reliability of avian molecular clocks is actually based on only a small number of calibrations carried out under different assumptions with respect to the choice and constraints of calibration points or to the use of substitution models. In this study, we provide substitution rate estimates for two mitochondrial genes, cytochrome *b* and the control region, and age estimates for lineage splits within four subgenera of tits (Paridae: *Parus*, *Cyanistes*, *Poecile* and *Periparus*). Overall sequence divergence between cytochrome *b* lineages covers a range of 0.4–1.8% per million years and is thus consistent with the frequently adopted approximation for a sequence divergence between avian lineages of 1.6–2% per my. Overall rate variation is high and encompasses the 2% value in a 95% CI for model corrected data. Mean rate estimates for cytochrome *b* range between 1.9 and 8.9×10^{-3} substitutions per site per lineage. Local rates differ significantly between taxonomic levels with lowest estimates for haplotype lineages. At the population/subspecies level mean sequence divergence between lineages matches the 2% rule best for most cytochrome *b* datasets (1.5–1.9% per my) with maximum estimates for small isolated populations like those of the Canarian *P. teneriffae* complex (up to 3.9% per my). Overall rate estimates for the control region range at similar values like those for cytochrome *b* ($2.7–8.8 \times 10^{-3}$, 0.5–1.8% per my), however, within some subgenera mean rates are higher than those for cytochrome *b* for uncorrected sequence data. The lowest rates for both genes were calculated for coal tits of subgenus *Periparus* (0.04–0.6% per my). Model-corrected sequence data tend to result in higher rate estimates than uncorrected data. Increase of the gamma shape parameter goes along with a significant decrease of rate and partly age estimates, too. Divergence times for earliest deep splits within tit subgenera *Periparus* and *Parus* were dated to the mid Miocene at 10–14 my bp. Most recent splits between east and west Palearctic taxa of blue, willow and great tits were dated to the Pliocene/Pleistocene boundary with the earliest estimates based on model-corrected trees. Relaxation of the Messinian calibration point leads to more recent divergence times for North African coal and blue tit populations during the mid Pliocene. Despite a relatively broad age constraint for the split between Nearctic and Palearctic Poecile due to the Pliocene re-opening of the Bering Strait, the split between chickadees and willow tits is dated considerably earlier than in former studies to the upper bound of the age constraint at 7.4 my BP.

Keywords: Molecular clock; Paridae; Cytochrome *b*; Control region; Substitution rates; Calibration points; Paleogeography; Age dating

1. Introduction

Among the increasing number of molecular phylogenetic studies on avian mitochondrial DNA, two genes, cytochrome *b* (CYTB) and the control region (CR), are

* Corresponding author.
E-mail address: Martin.Paeckert@snsd.smwk.sachsen.de (M. Päckert).

1055-7903/$ - see front matter © 2007 Elsevier Inc. All rights reserved.
doi:10.1016/j.ympev.2007.03.006

certainly the most common markers used for the reconstruction of molecular phylogenies and species delimitation. Mitochondrial sequence comparison was proven to be a useful tool for the detection of genetic differentiation from the population up to species and genus level. Particularly in those taxa showing great morphological homogeneity, cryptic species were determined by the aid of molecular methods, e.g. in old world warblers of the genera *Phylloscopus* and *Seicercus* (Martens et al., 1999; Irwin et al., 2001; Olsson et al., 2004, 2005; Päckert et al., 2004). Apart from taxonomic implications, nearly all assessments on avian radiations and timing of lineage splits were based on a postulated mitochondrial clock (Brown et al., 1979). Since this very beginning, rate estimates for the cytochrome *b* gene oscillate around 1.6–2% sequence divergence between lineages per million years, and accordingly this estimate soon became a reference value in ornithological molecular research. At the same time only a few molecular studies actually provided a reliable clock calibration and these mainly differed in the inference of calibration points. Calibrations on the fossil record, and accordingly dated by older evolutionary events, were applied to sequence data of geese (Shields and Wilson, 1987; Paxinos et al., 2002), cranes (Krajewski and King, 1996), albatrosses (Nunn et al., 1996; Nunn and Stanley, 1998), partridges (Randi, 1996) and of other galliform birds (Pereira and Baker, 2006). However, the fossil record is poor in many, especially younger avian lineages, and thus fossil dating is almost limited to avian orders and families but fails for clock calibration at the genus, species, or subspecies level. Therefore, a second category of molecular clock calibrations refers to paleogeographic ages, for instance of volcanic islands or geographic barriers. Such were used as calibration points for rate estimates in Hawaiian honeycreepers (Fleischer et al., 1998), ratites (Cooper et al., 2001), Macaronesian gold- and firecrests (Päckert et al., 2006), North American and Cuban Ivory-billed woodpeckers (Fleischer et al., 2006) and even at the family level for a large sample of passerine lineages (Barker et al., 2004).

With increasing knowledge of the avian mitochondrial genome, considerable doubts were cast on the "clocklike behaviour" of the frequently used marker genes and especially the 2% rule of thumb became the focus of a lively debate. So far, the discussion basically concentrated on the crucial comparability of clock calibrations based on different assumptions with respect to calibration points, the impact of saturation of substitutions and the use of uncorrected or model-corrected datasets (reviews in Arbogast et al., 2002; García-Moreno, 2004; Lovette, 2004; Ho and Larson, 2006).

Among passerine birds tits and titmice range among the best known and most intensely studied families. They are characteristic avian faunal elements of the entire Holarctic region with a hot spot of diversity in the Himalayan and Chinese mountain ranges. Several species radiated to the Oriental and the Afrotropical region, too. In the Australian and the Neotropical region tits are completely absent. The complex pattern of geographic distribution of several tit species was object to several phylogeographic studies with respect to radiation, vicariance and speciation processes (Gill et al., 2005; Martens et al., 2006; Kvist et al., 1999, 2001, 2003a,b, 2004, 2005; Kvist and Rytkönen, 2006; Päckert et al., 2005; Salzburger et al., 2002a,b). In a recent molecular study based on cytochrome *b* sequences of 40 tit species Gill et al. (2005) recommended the elevation of six parid genera from the respective classical subgenera. Here, we follow the traditional taxonomy with one parid genus *Parus* in accordance with Harrap and Quinn (1996) and Dickinson (2003).

In this study we provide estimates for substitution rates and times of divergence between mitochondrial lineages (cytochrome *b* and the control region) for several parid datasets: great tits: subgen. *Parus*; blue tits: subgen. *Cyanistes*; chickadees: subgen. *Poecile*; coal tits: subgen. *Periparus*. We use a non-parametric approach which takes into account rate heterogeneity among clades. The impact of substitution model settings, input tree reconstruction and of calibration point constraints on rate and age estimates is investigated by comparing different runs with uncorrected and model-corrected NJ and ML input trees and with different paleogeographic age constraints.

2. Materials and methods

2.1. Rate and age estimates

With respect to a proper definition of terms, it has to be emphasized, that the popular 2% rule for cytochrome *b* refers to a "sequence divergence between lineages" (given in percent per million years)—likewise it will be termed in the following. Substitution rates as estimated with r8s 1.70 refer to single mitochondrial lineages and are given in substitutions per site per lineage per time unit (subst./site/lineage/my).

For estimating absolute rates of molecular evolution in the control region and in cytochrome *b* and divergence times between different mitochondrial lineages of the subgenera *Parus*, *Cyanistes*, *Poecile* and *Periparus* we used the software package "r8s 1.70" (Sanderson, 2003, 2004). Molecular datasets largely originated from several previous studies (sequences available at GenBank; a full reference of accession numbers is given in the Supplementary material). We furthermore sequenced additional samples from great, blue and azure tits that were not included in the respective studies to broaden the sample range for these groups. PCR and sequencing were carried out according to the original publications (*P. major*: Päckert et al., 2005; Kvist et al., 2003b; *P.caeruleus* and *P. cyanus* Kvist et al., 2004, 2005). A total of 119 cytochrome *b* and 354 control region sequences were available for the reconstruction of input trees for the different subgenera.

2.2. GenBank Accession Nos.

Parus montanus–Parus atricapillus group, cytochrome *b*: AF396239–AF396259 (Salzburger et al., 2002b); control

region: AF354299-403, AF354495-98, AF275185 (Kvist et al., 2001).

Parus major–Parus monticolus group, cytochrome *b*: AY75557–AY75586 (Päckert et al., 2005); control region: AF542237-76, AF542279-358, AF542360-76, AF537962-89, AY136804-13 (Kvist et al., 2003a,b, 2007).

Parus caeruleus–Parus teneriffae group, control region: AY538186–AY538249, AY267083–AY267088, AY588282–AY588289 (Kvist et al., 2005); new sequences: DQ020317-47, DQ483095–DQ483108.

We furthermore used sequence datasets from current studies on blue and ultramarine tits (cytochrome *b*: Dietzen et al., in prep., GenBank Accession Nos: DQ474002–DQ474061, previously unpublished) and on coal tits and allies (GenBank Accession Nos., cytochrome *b*: DQ217844–DQ217901, Martens et al., 2006; control region: DQ466198-DQ466219, previously unpublished). Further sequences by Gill et al. (2005) were used for reconstruction of a molecular parid phylogeny including the most frequent cytochrome *b* haplotype of each taxon from our subgenus datasets (full reference of accession nos. in the Supplementary material). Altogether, we compared estimates from nine molecular datasets: both genes in each of the four subgenera plus the pooled cytochrome *b* data for all Paridae with each taxon represented by the most common haplotype. Sequences were aligned with BioEdit (Hall, 1999) and phylogenetic reconstruction of input trees was carried out with PAUP (Swofford, 2001).

To check the investigated datasets with respect to rate constancy we performed likelihood ratio tests with tree puzzle 5.5. (Schmidt et al., 2000). For eight of nine datasets the simpler clocklike tree was rejected on a significance level $p < 0.05$, thus rate constancy cannot be assumed for these sequence data (Table 1). Only for cytochrome *b* sequences of subgenus *Parus* (great tits and allies) log-likelihoods of the more complex tree (not clocklike) did not significantly increase, and thus indicated rate constancy for this dataset (compare Päckert et al., 2005). In order to test the significance of rate differences between clades, further relative rate tests were carried out with r8s 1.7. The relative rate test implemented with r8s is a likelihood ratio test of whether two or more clades descending from a particular node of the input tree are evolving at the same rate (r8s 1.70: command, ⟨*rrlike taxon = taxonname*⟩).

2.3. Input trees

For input in r8s 1.70 we reconstructed haplotype neighbor-joining trees (NJ, Saitou and Nei, 1987) and maximum likelihood trees (ML, quartet puzzling) with each haplotype represented once with PAUP (Swofford, 2001). Several runs with r8s were conducted with uncorrected and model-corrected input trees. For each dataset the best fit substitution model was estimated with modeltest 3.7. for windows (for model settings applied see Table 1). Additional ML input trees were reconstructed with default likelihood settings (which implied a less complex substitution model: HKY for all datasets with equal rates and a Ti–Tv ratio close to $k = 4$). All trees were reconstructed without enforcement of a molecular clock, thus branch lengths of input trees were not ultrametric, which requires an according command in r8s (⟨*ultrametric = no*⟩). Furthermore, to investigate the impact of the applied substitution model on rate and age estimates with r8s 1.70, we reconstructed several input trees (*P. major* cytochrome *b* data) differing in model settings with gamma-shape parameter α ranging from 0.3–1.0. Zero branch lengths were automatically collapsed and turned into hard polytomies (r8s 1.70, command: ⟨*collapse*⟩).

For rooting of trees we followed the recommendations for obtaining input r8s trees with branch lengths (Sanderson, 2004) and used an "extra outgroup taxon that is distantly related to all the remaining taxa". Cytochrome *b* phylogenies were rooted with two sequences of long-tailed tits (*Aegithalos concinnus*) as the more closely related and two further more distantly related outgroups (*Regulus regulus*, *Phylloscopus collybita*). Rooting of subgenera datasets was performed accordingly with the non-parid outgroups and two further parid sequences from a different subgenus. As one option recommended by Sanderson (2004) all distantly related outgroups were retroactively removed from the subgenus trees, so that the root node of each subgenus input tree was an internal node of the parid tree (in subgenus trees either European *P. caeruleus* or European *P. major* at the root node).

2.4. Paleogeographic age dating

For reconstruction of divergence times and absolute rates of substitution with r8s 1.70 we used non-parametric rate smoothing (NPRS method: Sanderson, 1997) which relaxes the assumption of a molecular clock on the basis of least squares smoothing of local rate estimates (Sanderson, 2004). Among the different algorithms available for finding optima of the objective functions, we chose POWELL algorithm (Press et al., 1992) which is recommended for constraint problems by the author (Sanderson, 2004). Several key nodes of the molecular input trees were constrained to age estimates for paleogeographic events which should roughly correspond to lineage splits between parid clades, i.e. ages of volcanic islands, rise of geographic barriers, submerging or emerging of land bridges etc. Island ages were already used as earliest constraints of the invasion of ancestral founder populations to a given island for the inference of mitochondrial substitution rates in several studies (Fleischer et al., 1998, 2006; Warren et al., 2003).

As time estimates for most events comprise time spans like oldest and youngest lava shields (available for all Canary islands) rather than a fixed point in time, several nodes of input trees were constrained to a minimum and a maximum age. We refer to five paleogeographic events that gave rise to geographic barriers or new habitats, for instance on volcanic islands, as calibration points.

Table 1
Model settings of substitution models estimated with modeltest 3.7 and results from likelihood ratio tests with tree puzzle 5.5. for all tit data sets

Data set	log L1	log L2	model	I	Gamma	Base frequency	Rate matrix	Ti/Tv ratio
Parus cyt*b*	−1710.07	−1734.71	HKY+I+G	0.6421	1.1079	27.33 36.39 13.83 22.45	—	3.3874
Cyanistes cyt*b*	−2499.99	−2528.27*	TVM+I+G	0.6107	0.3842	27.99 37.11 12.59 23.31	1.9577 17.1739 0.4010 0.0000 17.1739	—
Poecile cyt*b*	−980.10	−995.75*	TVM+I	0.7069	—	25.09 36.18 14.91 23.81	—	—
Periparus cyt*b*	−2531.35	−2582.74*	TRN+I+G	0.4791	0.5502	27.57 36.11 14.10 22.22	1.0000 17.5296 1.0000 1.0000 12.2294 1.0000	—
Paridae cyt*b*	−7028.15	−7680.27*	TVM+I+G	0.5377	0.9195	0.3221 0.3709 0.1166 0.1904	0.7530 8.1451 1.2624 0.1811 8.1415 1.0000	—
Parus cr	−2684.14	−2882.71*	TRN+I+G	0.3856	0.7025	26.27 30.76 16.11 26.86	1.0000 10.0173 1.0000 1.0000 4.5686 1.0000	—
Cyanistes cr	−2832.05	−2950.16*	TIM+I+G	0.4994	0.6555	28.14 29.45 16.28 26.13	1.0000 6.0314 0.6720 0.6720 3.2284 1.0000	—
Poecile cr	−2562.97	−2861.48*	HKY+I+G	0.6594	0.8532	25.71 30.01 17.69 26.58	—	8.4509
Periparus cr	−2606.49	−2725.79*	TVM+I+G	0.4464	0.6991	26.44 26.45 19.55 27.65	0.4007 1.4249 0.2320 0.8246 1.4249 1.0000	—

* The simpler clocklike tree was rejected on the $p < 0.05$ level.

2.5. Ages of volcanic islands

(1) El Hierro: 1.12 my bp (Guillou et al., 1996)
(2) La Palma: 1.77 my bp (Ancochea et al., 1994)

Both values were used as maximum age constraints as earliest possible time of invasion of Canarian ultramarine tits to the respective islands.

2.6. Continental events

(3) Recent split between Nearctic and Palearctic faunal elements (willow tits and chickadees) initiated by the last Pliocene opening of the Bering Strait 4.7–7.4 my ago (Marincovich and Gladenkov, 1999); used as maximum and minimum age constraint.

(4) Separation between ancestors of east and west Palearctic faunal elements: Beginning of the Pleistocene traditionally refers to an increase of cryophilic nanoplankton at 1.7 mya (Aguirre and Pasini, 1985), first cold periods, continental ice shields and decline of tertiary forests earlier about 2.4 my BP (West, 1988); both values used as maximum and minimum age constraint. East and southeast Asian late Pleistocene refuge areas of forest dwelling birds already matched their recent distribution (Nazarenko, 1988). Separation of nowadays allopatric east and west palearctic metapopulations of the azure-winged and the common magpie (*Cyanopica cyanus*, *Pica pica*) was dated to the late Pliocene/Pleistocene boundary by mitochondrial sequence data (Kryukov et al., 2004).

(5) Split between continental European and North African populations initiated by the re-opening of the Strait of Gibraltar at the end of the Messinian crisis 5.32–5.96 BP (Gautier et al., 1994; Krijgsman et al., 1999); both values used as maximum and minimum age constraint.

For the significance of the Messinian crisis for faunal interchange between southern Europe and North Africa see: Veith et al., 2003, 2004; Griswold and Baker, 2002; Godoy et al., 2004.

All five calibration points were used for the pooled cytochrome *b* dataset with respect to the following key nodes.

Cyanistes: key nodes: *Parus teneriffae ombriosus* vs. Canarian sister clade, cal. point 1; *P. t. palmensis* vs. all remaining ultramarine tits, cal. point 2; split between ultramarine and European blue and azure tits, cal point 5.

Parus: key node: split between east and west Palearctic clades of great tits (*P. m. major*/ *P. m. bokharensis* vs. *P. minor*/ *P. cinereus*), cal. point 4.

Poecile: key node: split between North American chickadees (*P. atricapillus*/*P. carolinensis*) and Eurasian marsh and willow tits (*P. palustris*/*P. montanus*), cal. point 3.

Periparus: key node: North African *P. ater atlas* vs. its remaining Eurasian coal tit sister clade, cal. point 5.

Accordingly, rate calibrations for subgenus datasets were based on one up to three calibration points for ingroup nodes. We did not make use of additional outgroup nodes (e.g. from a different parid subgenus), since the use of external calibration points might lead to a considerable underestimation of ingroup node ages (Pereira and Baker, 2006; Ho and Larson, 2006).

95% confidence intervals for age estimates, e.g. for parid subgenera, were calculated according to the built-in strategy of r8s recommended by Sanderson (2004) to be included in the divtime command:

divtime method = nprs confidence = yes taxon = ⟨subgenus⟩ cutoff = 4

With respect to the possible existence of multiple local optima, r8s provides a multiple starts function to ensure that a global optimum of rate estimates is reached. We performed multiple starts with the pooled Paridae data under the following settings:

set num_time_guesses = n seed = 1; with $n = 5$ and $n = 10$ perturbations.

Mean rate estimates from one start and five start searches differed by only 0.00009–0.0002 subst./site/lin./my. Rate estimates from five and ten start searches were exactly the same.

Nexus input files based on ML input trees (default model) for each dataset are provided in the Supplementary material.

Differences between mean rate estimates for different populations and levels of mtc divergence were analysed with SPSS 12.0 (including further statistics like linear regression, *T*-tests, non-parametric tests, etc.).

3. Results

3.1. Mean and local rate estimates

Mean substitution rate estimates for parid cytochrome *b* range between 1.9×10^{-3} and 8.9×10^{-3} substitutions per site per million years (lowest in *Periparus* and highest in *Cyanistes*) depending on the method and the application of substitution models for input tree reconstruction (Table 2). These estimates roughly equal an approximate genetic distance between mitochondrial lineages of 0.4% and 1.8% (Table 2). Overall rate estimates for the control region cover nearly the same range as those for cytochrome *b* (0.5–1.3%). In most runs the highest rates are observed for the *Cyanistes* datasets ($5.9–8.9 \times 10^{-3}$) equalling a mean sequence divergence between blue tit lineages of 1.2% and 1.8%. Lowest rates for both genes were found in subgenus *Periparus* and covered a range between 0.2 and 3.2×10^{-3} (0.04% and 0.6%). The same mean and local rate differences between the four tit subgenera resulted from runs with the pooled CYTB dataset (highest rates in *Cyanistes* lowest in *Periparus*, Table 2).

For uncorrected input data CR rates tend to be equal or higher than CYTB rates, while most model-corrected datasets yielded equal or lower rates in the control region. In subgenus *Poecile* all estimates for CR rates yielded lower values than for CYTB.

With respect to the levels of genetic divergence, minimum rate estimates are yielded for terminal branches of the input trees, while rate estimates for the deeper branches generally range at higher values. Mean local rates of haplotype lineages range between 2.6 and 5.2×10^{-3} in cytochrome *b* while among population and subspecies lineages local rates range at higher values between 4.2×10^{-3} and 1.0×10^{-2}. To check for differences between mean local rates at different levels of genetic divergence we divided our estimates into four categories (Fig. 1): rates of (1) terminal clades (haplotypes), (2) clades within haplotype clusters, (3) species or subspecies lineages, e.g. Canary island clades, subspecies sectors of *P. major* etc., (4) deeper clades, e.g. connecting sister taxa. *T*-tests were carried out for pooled rate estimates of each of the four categories

Table 2
Rate estimates for cytochrome *b* and control region datasets of four subgenera of tits and the pooled cytochrome *b* dataset (members of all subgenera, range of local rates)

Mtc gene	Cytochrome *b*				Control region	
	Mean rate		%		Mean rate	%
Input tree	Subgenus	Pooled	Subgenus	Pooled	Subgenus	
Parus	6.1	1.6–12.0	1.2	0.3–2.4	6.3	1.3
Cyanistes	7.0	2.0–22.0	1.4	0.4–4.4	6.0	1.2
Poecile	5.1	2.0–6.8	1.0	0.4–1.4	3.0	0.6
Periparus	0.2	1.1–4.0	0.04	0.2–0.8	3.2	0.6
Paridae		5.9		1.2		

Estimates inferred from runs with ML input trees (simple model: HKY with equal rates and Ti–Tv ratio of about 4); mean rate $\times 10^{-3}$ given in subst./site/lineage/my; %: sequence divergence between lineages given in % per my.

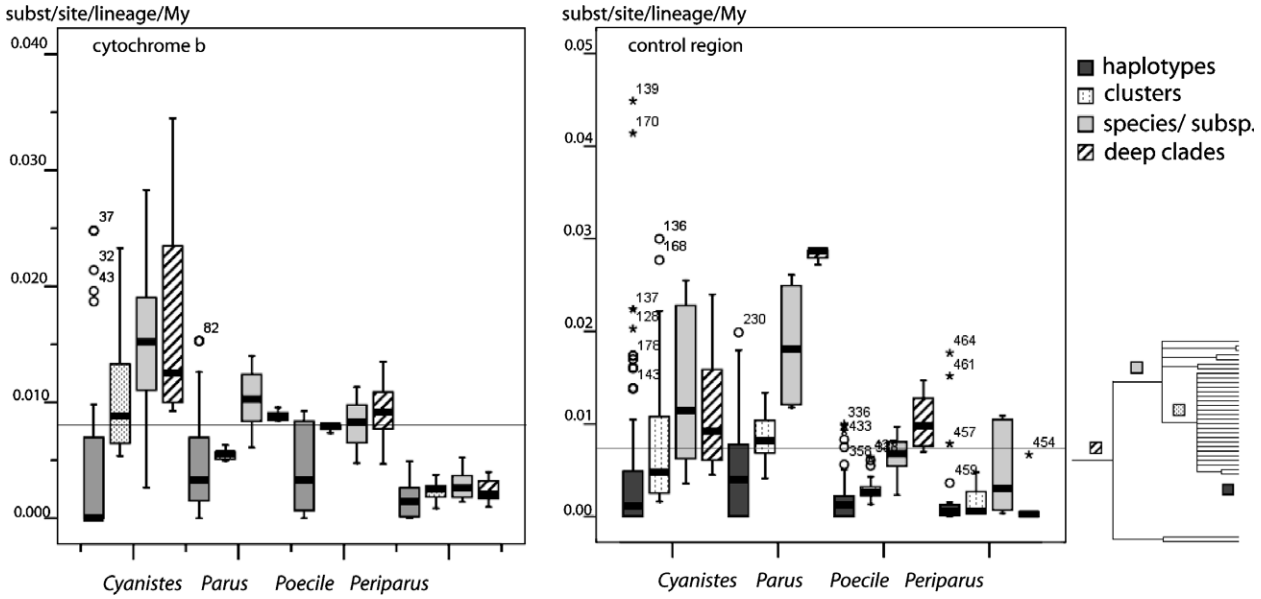

Fig. 1. Boxplot of mean local rates of cytochrome *b* and the control region at four different levels of genetic divergence within tit subgenera; bars: median, boxes: quartile, whiskers: 95% CI; divergence levels: (1) haplotypes = terminal clades; (2) clusters = clades within haplotype clusters; (3) species and subspecies lineages; (4) deep clades connecting sister taxa or sister taxon groups; estimates based on model corrected NJ input trees; the rate estimate by Fleischer et al. (1998) of 0.008 subst./site/lin./my is indicated by horizontal lines.

against those of the next higher level of genetic divergence. Despite a large range of estimates especially in *Cyanistes*, model-corrected rates increase significantly with the level of genetic divergence for most datasets except cytochrome *b* in *Poecile* and both genes in *Periparus* (Fig. 1). In *Cyanistes* and *Parus* CTYB rates are significantly higher for species/subspecies lineages than rates at the population level (terminal clades vs. categories 2 and 3 in *Cyanistes*, and clades within haplotype clusters [cat. 2] vs. those of subspecies/ species lineages [cat. 3] in *Parus*, *T*-test, $p < 0.05$). Control region rate estimates increase significantly with divergence level between terminal clades, haplotype clusters and species lineages in *Cyanistes* and *Parus* and *Poecile* (*T*-test, $p < 0.01$; in *Poecile* significant differences only between haplotype lineages and clusters and species lineages but not within haplotype clusters). For uncorrected input data the estimate by Fleischer et al. (1998) lies beyond the 95% confidence interval in all subgenera at almost each level of divergence except in *Cyanistes*. However, model-corrected input trees yield a slight increase of rate estimates, so that 95% CI embrace the value by Fleischer et al. (which was based on K2 model-corrected sequence data) in every subgenus except *Periparus* (Fig. 1). In both genes rate estimates for the latter group range at lower values at all levels of divergence for model-corrected data, too! Unlike for CYTB sequence data, in the latter two subgenera some terminal branches of CR trees reach maximum rate estimates: in *Periparus* highest among haplotypes of the southern European *abietum* clade and among those of the Nepalese *melanolophus* clade (1.0×10^{-2}–1.8×10^{-2}); in *Poecile* highest within the *songarus* clade and the *restrictus* clade from Japan; 5×10^{-3}–9×10^{-3}).

3.2. Rate variation among clades at the same taxonomic level

Local rates at the species/subspecies level do not considerably differ within tit subgenera except among blue and

ultramarine tit lineages. In subgenus *Cyanistes*, maximum estimates were yielded for the Canarian clades of the *P. teneriffae* group and range from 1.0×10^{-2} up to 1.6×10^{-2} (Figs. 2 and 3). Local rates of Canarian ultramarine tit populations differ significantly from local rates of continental blue and azure tit clades by about one decimal power in both genes for uncorrected and corrected data (*T*-test, $p < 0.05$, for pooled estimates of island vs. continental clades, but not for island vs. continental haplotype lineages; Fig. 3). The entire Canarian sister clade to *P. teneriffae palmensis* from La Palma yielded the highest local CR rate of all runs (5.3×10^{-2}) due to a 12 bp indel shared by all Canarian populations except the one from La Palma (Fig. 2). A likelihood ratio test implemented with r8s confirmed that CYTB rates within the entire *Cyanistes* clade and within the inner Canarian clade (*ombriosus* vs. *teneriffae/ultramarinus*) differ significantly ($\log L1 = -100.58$, $\log L2 = -93.14$; $\log L1 = -44.85$, $\log L2 = -44.12$; both $p < 0.05$). CR rates differ significantly within the Canarian clade between *palmensis* and all other Canarian populations (-145.23, $\text{Log}\,L2 = -134.16$; $p < 0.01$). In contrast, in both genes rates among the continental clades of *P. caeruleus* and *P. cyanus* did not differ significantly neither did local rates within the main Canarian clade in the control region (*palmensis* from La Palma excluded).

Though also within *Poecile* high local rates were found in terminal clades of populations with a small distribution range, the pooled estimates from these island populations (Sakhalin and Japan) and of *P. songarus* did not differ significantly from local rates in widely distributed continental populations. The same holds true for blue tits from Corsica (Fig. 2).

At the species/subspecies level rate estimates equal a sequence divergence between parid CTYB lineages between 1.5 and 1.9% per million years within *Parus, Poecile* and *Periparus* and up to 3.9% per million years within *Cyanistes*. Rate estimates for the pooled CYTB dataset again yielded the highest values in the Canarian ultramarine tit clades (*P. teneriffae*; 0.6×10^{-3}–1.8×10^{-2} subst./site/lineage/my; 1.2–3.6% per my) while for all other main lineages of the parid tree rate estimates range at lower values from 3×10^{-3} to 5×10^{-3} subst./site/lineage/my (0.6–1.0% per my).

3.3. Impact of substitution model

For all datasets, model-corrected input trees lead to slightly divergent rate estimates with r8s 1.70 compared to those inferred from uncorrected trees. In most runs, model-corrected datasets yielded higher mean and local rates with the exception of subgenera *Cyanistes* and *Periparus* for which runs with the more complex ML trees model resulted in considerably lower estimates. Rate estimates inferred from ML input trees differ significantly from those inferred from NJ input trees for *Cyanistes*, *Poecile*, *Periparus*, but not for *Parus* (model-corrected data, *T*-test, $p < 0.01$). Estimates inferred from different ML input trees (simple and complex model) differ significantly only for

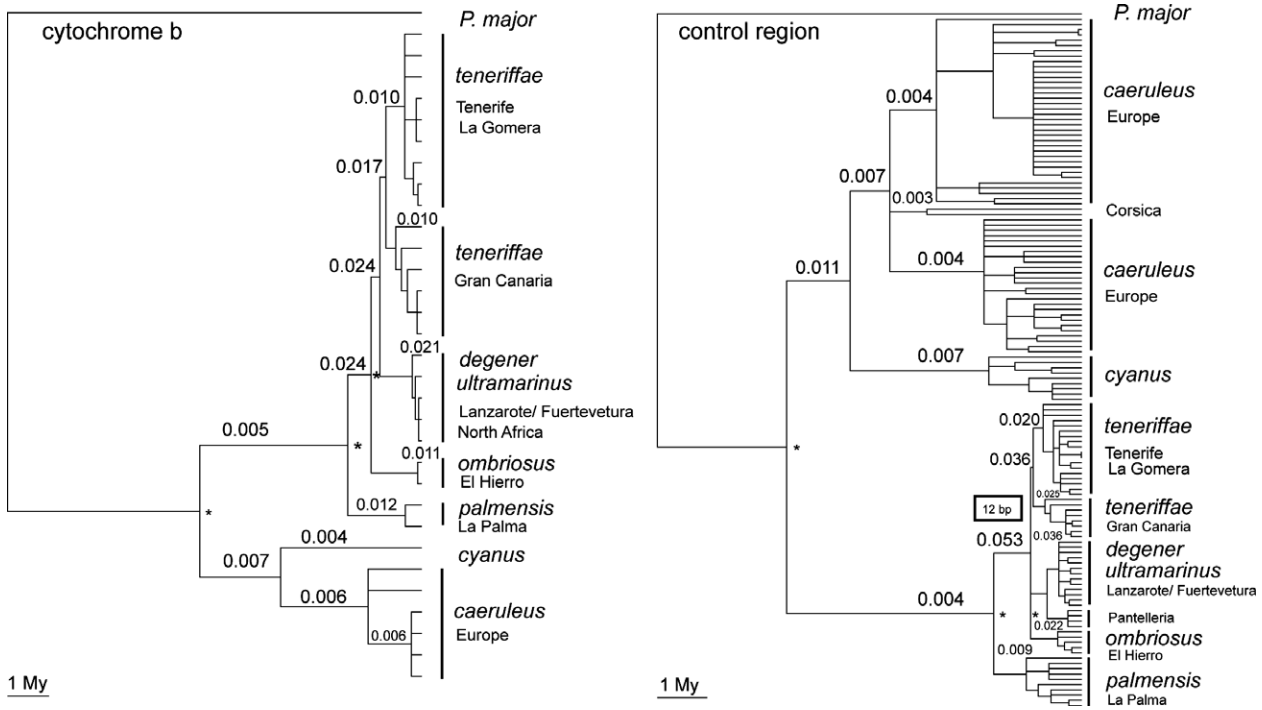

Fig. 2. Mitochondrial clocktrees (ML, quartet puzzling) for cytochrome *b* (1005 bp) and the control region (504 bp) in subgenus *Cyanistes*; local substitution rates indicated above branches (substitutions per site per lineage per million years); * = calibration points; a deletion of 12 bp in domain II of the control region is shared by all Canary islands populations except *P. teneriffae palmensis* from La Palma (highest local rate, deletion indicated above branch).

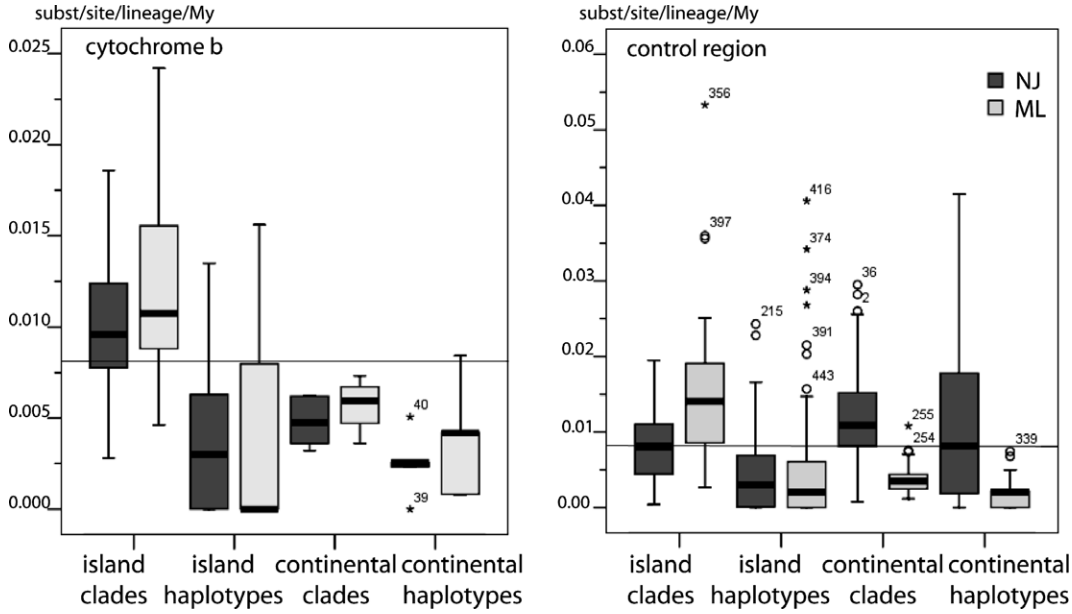

Fig. 3. Boxplot of mean local rates of cytochrome *b* and the control region in continental and island populations of blue tits (subgenus *Cyanistes*); bars: median, boxes: quartile, whiskers: 95% CI; estimates compared for corrected NJ and ML input trees; the rate estimate by Fleischer et al. (1998) of 0.008 subst./site/lin./my is indicated by horizontal lines.

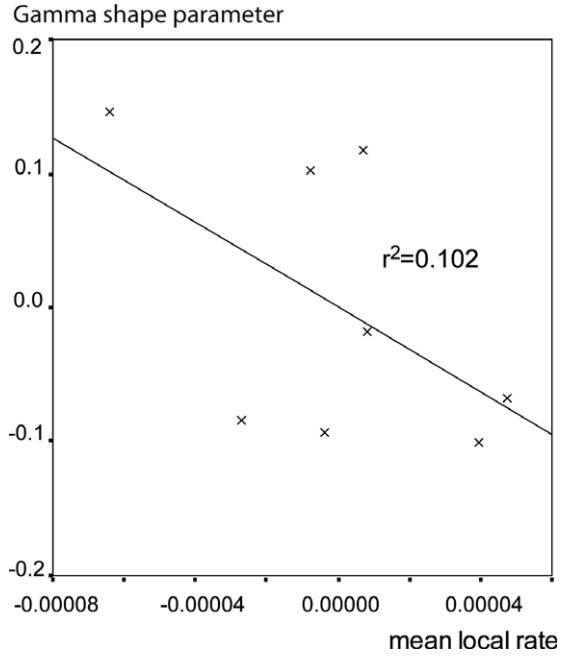

Fig. 4. Linear regression for correlation of the gamma shape parameter with mean local rate estimates; rates and ages standardized.

Cyanistes (*T*-test, $p < 0.01$). In blue and ultramarine tits this effect is certainly due to the collapse of the main blue tit lineages to a basal trichotomy in the model-corrected ML tree (Eurasian, Canarian and La Palma clade) which required a relaxation of the two basal calibration points 2 and 3 and the concurrently alternate position of *P. t. ombriosus* (calibration point 1) to a more recent node. Likewise, in *Periparus* the position of *P. a. atlas* alters in both ML trees, so in both cases low rate estimates for the more complex model are probably an effect of the displacement of calibration nodes. However, a relaxation of the Messinian calibration point to only a maximum age of 5.96 my allowing to shift the divergence time between North African and European coal tits to more recent ages does not lead to markedly different rate estimates even for corrected ML input data. Results from modified calibrations differ by a sequence divergence of only 0.1–0.2% per my.

Further impact of the substitution model on rate and divergence time estimates is evident from subsequent runs of r8s with various input trees (subgenus *Parus*) differing in gamma shape parameter α. With increasing α within the given range from 0.3 to 1.0 rate estimates for cytochrome *b* tend to decrease about 5.7×10^{-4} (Fig. 4; $r^2 = 0.102$). This correlation is not significant for the entire test range of α, however, within a given range of $0.3 < \alpha < 0.7$ mean rates decrease significantly ($r^2 = 0.858$; ANOVA, $p < 0.05$). Age estimates for the divergence time between *P. major* s.l. and *P. monticolus* decrease significantly with increasing α within the given range ($r^2 = 0.630$; ANOVA, $p < 0.05$). However, a slight increase of the age estimate for the split between the subspecies groups *major* and *bokharensis* with increasing α is significant only within the restricted range of $0.3 < \alpha < 0.7$, too ($r^2 = 0.755$; ANOVA, $p < 0.05$).

3.4. Age estimates

Age estimates based on all five calibration events for the pooled CYTB data suggest that early radiation events within subgenera *Parus* and *Periparus* occurred in the

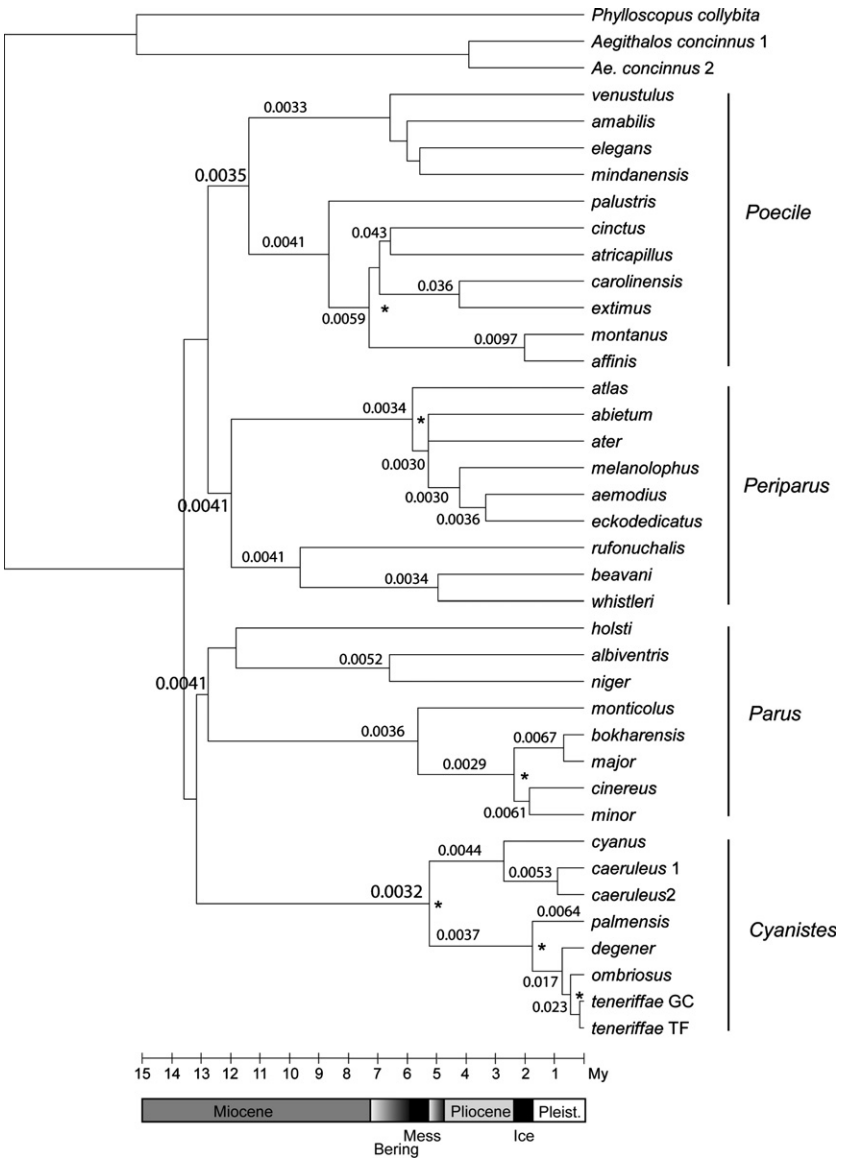

Fig. 5. Mitochondrial clocktree (NJ model-corrected) for pooled Paridae dataset (based on 614 bp cytochrome *b*); *, nodes used as calibration points; mean local rate estimates indicated for main clades; time spans between maximum and minimum age constraints of three calibration points indicated in geological timescale: Bering, opening of Bering Strait; Mess, Messinian salinity crisis; Ice, beginning of Pleistocene (Pleist.).

upper Miocene between 9 and 12 my BP (splits between African grey and Palearctic great tits, and between coal tits, rufous-naped and rufous-vented tits, Table 3, Fig. 5). Most recent splits between tit populations have occurred in the northern Palearctic range during the late Pleiocene (separation of blue and azure tits) and during the Pleistocene (isolation of *P. songarus affinis*, *P. bokharensis* antecendants and separation of two European blue tit clusters; Table 3, Fig. 5). For the latter more recent splits estimates based on ML corrected input trees yielded slightly older ages between 0.7 and 3.9 my BP, while estimates for deeply divergent splits like among members of *Periparus* are younger for model-corrected data than for uncorrected data (Fig. 4). Age estimates based on control region sequence data are considerably higher (up to twice as much as CYTB estimates) for the more recent radiations of willow, blue and great tits (Table 3).

Relaxation of calibration point 5 (Messinian crisis) to a maximum age constraint of 5.96 my (no minimum age) resulted in younger age estimates for several lineage splits within *Parus* (while mean rate estimates only slightly increased). Without a minimum age constraint for the European/ African split the North African coal tits, *P. ater atlas*, were estimated an older lineage (4.2 my ago) than North African and Canarian blue tits, *P. teneriffae* (3.2 my ago). In runs with subgenus datasets, alteration of the Messinian calibration point leads to more recent age estimates within *Cyanistes*, too (split of African/Canarian taxa from European *caeruleus* clade at 2.66 my ago), but to much higher age estimates between main *Periparus*

Table 3
Age estimates for tit clades inferred from pooled cytochrome *b* sequences in my BP; 95% confidence intervals calculated via built-in procedure included in divtime command of r8s; input trees (NJ: substitution model estimated with modeltest; ML: simple HKY model; ML corr: more complex substitution model estimated with model test

clade	NJ	95% CI	ML	95% CI	ML corr	95% CI
Parus	11.7	[10.6–14.0]	—	—	9.0	[7.4–10.0]
Periparus	11.0	[10.0–13.5]	11.9	[10.2–16]	10.7	[9.7–12.6]
Poecile	8.6	[8.2–9.2]	7.3	[4.2–7.4]*	7.3	[4.2–7.4]*
rufonuchalis/rubidiventris	8.8	[7.5–10.8]	8.4	[6.7–11.6]	8.6	[7.5–10.0]
montanus/affinis	2.1	[1.8–2.4]	1.0	[0.7–1.5]	0.7	[0.6–1.1]
caeruleus/cyanus	3.0	[2.2–3.4]	3.1	[2.6–3.7]	3.9	[3.5–4.2]
caeruleus Europe	0.9	[0.6–1.5]	0.9	[0.7–1.4]	1.1	[0.8–1.5]
major/bokharensis	0.7	[0.6–0.9]	0.6	[0.5–0.8]	1.3	[1.3–1.4]

* An age constrained was assigned to this node during the respective run.

lineages (four different alterations with a most recent age estimate for the basal split between the *rufonuchalis/rubidiventris* clade and the *ater/melanolophus* clade at 15.7 my ago).

4. Discussion

4.1. Molecular clock calibration—influences

Despite a growing number of molecular clock calibrations for bird taxa and though several of these recent studies and reviews argue that the presumed avian mitochondrial clock is a much more complex phenomenon than formerly considered, the 2% rule of thumb is still a widely and frequently used tool for age dating in molecular systematics. Probably the most frequently referenced estimate of a mean sequence divergence between avian cytochrome *b* lineages of 1.6% per my originated from a clock calibration on Hawaiian honeycreepers by Fleischer et al. (1998). A more recent study from the same lab mainly confirmed this estimate with a clock calibration for North American and Cuban Ivory-billed woodpeckers, *Campephilus principalis* (1.9% per my; Fleischer et al., 2006). Basically, our results support these estimates with an overall mean sequence divergence between most tit cytochrome *b* lineages ranging from 0.7 to 1.8%. Since rate variation within most datasets is quite large, the estimate by Fleischer et al. (1998) is included in 95% confidence intervals of most mean rates from runs with model-corrected input data except within *Periparus* (lower mean rates for uncorrected and corrected data). In general, these rate differences between subgenera must be carefully interpreted, since they resulted from different calibrations based on different input trees and calibration points, which certainly is a potential source of error. However, we found the same differences between subgenera with rate estimates based on the pooled CYTB dataset (*Cyanistes* highest, *Periparus* lowest rates; the same calibration), so the overall variation and magnitude of substitution rate estimates among the four tit subgenera should be reliably reflected by these calibrations.

Overall mean sequence divergence between control region lineages covers nearly the same range as in cytochrome *b* (0.5–1.8%), however, mean CR rates tend to be slightly higher for uncorrected and slightly lower for corrected data—with the exception of subgenus *Poecile* which has considerably lower mean CR rates in all runs. Compared to cytochrome *b* the non-coding control region was shown to cover a broader range of substitution rates among different avian taxa and evolving on the average at a sequence divergence between lineages of 0.1 and 21% per my (Ruokonen and Kvist, 2002). Equal or slower rates in the control region (as inferred from model-corrected tit sequences) were also confirmed for Goldcrests (Päckert et al., 2006) and for curassows, Cracidae (Pereira et al., 2004). Crochet and Desmarais (2000) showed that within gulls average substitution rates in domains II and III of the control region and in cytochrome *b* range at roughly the same level, too, but also provided evidence for a decrease of rates in the usually faster evolving domain III due to secondary structures that might play a role in sequence conservation. For higher rates of the control region compared to CYTB in Old world warblers of the genus *Phylloscopus* see Irwin et al. (2001, up to 5% sequence divergence per my).

4.2. Calibration points and age estimates

Despite seemingly good congruence with former studies, our results also confirm the considerable impact of several calibration parameters on mean and local rate and time estimates. As a matter of fact, the calibration of a molecular clock based on paleogeographic events is substantially influenced by the choice and the constraints of calibration points. Calibrations based on younger (mainly paleogeographic) events were shown to result in faster molecular clocks than those based on older events like fossil record (Warren et al., 2003; García-Moreno, 2004). Accordingly, alteration of age constraints for single calibration points used in our study leads to different estimates of evolutionary divergence times between parid mitochondrial lineages, but results from modified calibrations show only minor differences in mean rates and sequence divergence.

Regardless of model correction, age estimates as inferred from pooled CYTB data suggest an origin of early parid radiation in the late Miocene between 7.4 and 14 my BP within subgenera *Periparus* and *Parus*. The more recent

splits between between east and west Palearctic vicariants were dated close to the Pliocene/Pleistocene boundary with earlier estimates from model-corrected data for Blue and azure tits. With respect to North African and Canarian tit populations, relaxation of the Messian calibration point with an unfixed minimum age results in younger estimates for coal tits (*P. ater atlas*) and ultramarine tits (*P. teneriffae* complex) during the Zanclean stage of the Pleiocene. In a few other bird taxa North African populations were suggested to have originated from more recent invasions indicating that the Strait of Gibraltar was not a major barrier in these species (Hewitt, 2004). According to our subgenus *Parus* dataset, divergence time of North African *P. major excelsus* from continental great tit populations was dated even younger at roughly 1 my BP suggesting that these populations originated from a Mediterranian Pleistocene refuge.

In contrast, the relatively broad time constraint for the split between Nearctic and Palearctic *Poecile* was always dated close to the maximum age constraint of 7.4 my BP, so that age estimates for the basal split within *Poecile* from several runs range at even lower values (8.0–9.2 my BP for a topology with *P. palustris* as sister to a clade of willow tits and chickadees). Despite the broad age constraint for the re-opening of the Bering Strait our estimates for the early radiation of North American *Poecile* are almost twice as high as those inferred from the 2% rule by Gill et al. (2005). We, therefore, have to keep in mind, that although our overall mean rate estimates for cytochrome *b* do match the 2% rule within a large range of variation between clades and taxonomic levels, the according age estimates for certain nodes (especially for constrained nodes) still may differ considerably from those calculated by rule-of-thumb.

Molecular data suggested an early origin of radiation—prior to a commonly suggested late Pleistocene origin of holarctic bird species–for several large passerine genera (New world warblers, *Dendroica*: Lovette and Birmingham, 1999; old world warblers, *Seicercus*, *Phylloscopus*: Irwin et al., 2001; Martens et al., 2004; Päckert et al., 2004). A similar evolutionary scenario was traced for brown frogs (Ranidae) on the base of mitochondrial and nuclear markers suggesting a late Miocene basal split between Palearctic and Nearctic clades and subsequent allopatric speciation triggered by climatic oscillations (Veith et al., 2003).

4.3. Application of substitution models

On the average model-corrected input trees yielded higher rate estimates than uncorrected trees and estimates of divergence times based on uncorrected data are mostly younger than for model-corrected input data. In a critical review of mitochondrial clocks Arbogast et al. (2002) already pointed out that age estimates based on under-corrected genetic distances (e.g. using uncorrected sequence data, *p*-distance) tend to be underestimated for dates younger and overestimated for dates older than the calibration point. Accordingly, in great and green-backed tits (*P. major*/*P. monticolus*) at low (e.g. underestimated) values of gamma ($\alpha < 0.7$) our age estimates for the younger split increase significantly with increasing α while estimates for the older Pliocene split decrease significantly (note, that a likewise high gamma shape was evaluated for these data: $\alpha = 0.9302$; Päckert et al., 2005). The impact of model correction on rate and age estimates has become one of the central arguments in the discussion on molecular clocks, and this aspect of the topic is clearest in the controversy over the late Pleistocene origin of species (Klicka and Zink, 1997; Arbogast and Slowinski, 1998; Johnson and Cicero, 2004). Yet, in the frequently adopted calibration by Fleischer et al. (1998) slightly lower rate estimates resulted from J–C-corrected sequence data compared to K2-P gamma-corrected data. Referring to that study, Warren et al. (2003) pointed out, that divergence times between sunbird clades (Nectariniidae) inferred from the 2% thumb rule deviated more or less considerably from those estimated with r8s under the different substitution models they applied to their data (absolute distances, ML distances and K2- distances as used by Fleischer et al., 1998).

4.4. Rate variation between levels of divergence

With respect to the taxonomic level investigated, local rate estimates show large differences between levels of genetic divergence, e. g. in cytochrome *b* low rates were estimated for terminal branches (within-population level) and higher rates for deeper branches (subspecies/ species level). Different percentages of replacement substitutions between levels of divergence resulted from a recent molecular study on great and willow tits by Zink (2005). His results suggest a significant decrease of replacement substitutions at the base of haplotype trees compared to tip clades and selection against this kind of substitutions over evolutionary time (Zink, 2005). Accordingly, the amount of genetic variation included in the investigated dataset has to be considered another highly influencing factor on rate and age estimates to keep in mind when comparing different clock calibrations. Since most avian clock calibrations were based on cytochrome *b* input trees using a single haplotype per taxon, we would expect these to result in mean rate estimates which roughly correspond to those yielded for the species/subspecies level in our study (category 3). On the average local rate estimates at this taxonomic level even lie above the mean estimates for each of the four tit subgenera ($0.8–1.5 \times 10^{-3}$, 1.6–3% per my except low values in *Periparus* of 0.3×10^{-3}, 0.6% per my). The underlying phylogenies of Fleischer et al. (1998) did not include any variation within populations either, but the results were controlled for intra-population variation (0.8×10^{-3}, 1.6% per my; see also Fleischer et al., 2006). Contrarily, studies including genetic variation at lower (intra-population) divergence levels yielded lower estimates for cytochrome *b* (Päckert et al., 2006; mean: 0.6–0.8% per my, but up to 3.6% between species/ subspecies lineages).

4.5. Variation of local rates between populations

In recent literature there is mixed support for accelerated mitochondrial substitution rates in small isolated populations as was confirmed for our Canarian ultramarine tit data. Johnson and Seger (2001) found an increase of rates in cytochrome *b* and ND2 from island populations of dabbling ducks (genus *Anas*) and doves (genus *Zaidura*) presumably due to an accumulation and fixation of non-synonymous substitutions. In addition, genetic drift is another probable elicitor of high mutational rates in small populations and was shown to have a significant impact on the genetic structure of avian island populations (Bollmer et al., 2005). In contrast, Bromham and Woolfit (2004) did not find evidence of an accelerated molecular clock due to adaptive island radiations by comparison of 19 vertebrate and invertebrate taxa. Nevertheless, the "island effect" is corroborated by significantly higher local rates in the Canarian ultramarine tit populations compared to the continental blue and azure tits for both genes. Accordingly, sequence divergence between Canarian lineages ranges between 2.0 and 4.2% per my. The maximum rate estimate from all runs for the Canarian ultramarine tit clade is certainly due to to a 12 bp deletion in domain II of the control region which is shared by all Canarian populations except the one from La Palma (*P. teneriffae palmensis*, 6.2% sequence divergence per my between the two Canarian clades). Generally, the influence of indels on population genetic analyses of vertebrate control region sequences appears to be small at the intraspecific but marked at the interspecific level (Pearce, 2006). Sequence divergence between ultramarine tit lineages over evolutionary time compares to estimates from a clock calibration for island sunbird populations (Nectariniidae) from the Comoros (cytochrome *b*: about 5.6%; Warren et al., 2003). Likewise, in goldcrest populations from the Azores, the Canary islands and Japan cytochrome *b* was shown to evolve at higher local rates than in continental populations, but this effect was not confirmed for the control region (Päckert et al., 2006).

In contrast, island populations of willow tits (*P. montanus*) and the narrowly distributed continental songar tits (*P. songarus*) show no significant acceleration of overall substitution rates, though in single haplotype lineages high local rates occured. Unlike Canarian ultramarine tits, Asian willow tits in Japan (*P. m. restrictus*) and on Sacchalin (*P. m. sacchalinensis*) evidently originated from a very recent late or even post Pleistocene radiation in the northern Palearctic (Kvist et al., 2001; Salzburger et al., 2002b), and the same holds true for the relatively young Mediterranian great tit populations on Corsica, *P. major corsus*(Kvist et al., 2003b). During this relatively short evolutionary time span the respective populations might have undergone fewer fluctuations of size with the according bottlenecks and drift effects than *P. teneriffae* populations on the Canary islands during approximately two my of geographic isolation. Second, and more important recent gene flow between continental Siberia and the Japanese archipelago and Sacchalin via a land bridge during late glacial maxima (Nazarenko, 1988) is reflected by two separate willow tit CR lineages from Japan and three from Sacchalin (Kvist et al., 2001). Thus, the unexpectedly low rate estimates for the respective populations might probably be due to the short and incomplete geographic isolation of willow tits on these islands.

Acknowledgments

The sequences used for this study were inferred from genetic material collected during regular field trips in C Europe and several expeditions of members of the three associated labs to Kirghizia/ Kazachstan (1993), Nepal (1995, 2001), China (1997, 1998, 1999, 2000, 2002; all J.M.); to the Canary islands (2001, 2002; C.D.), (2003; L.K. and M.P.); Far East Siberia and Japan (1996; M.P.).

Travel and research funds have been granted by the Forschungskommission, Deutsche Ornithologen–Gesellschaft (various grants, among them the E Asia grant to A. Gebauer, M. Kaiser and J.M.), the Gesellschaft für Tropenornithologie (J.M.) and by Feldbausch–Stiftung and Wagner-Stiftung, both at Johannes-Gutenberg-University, Mainz (J.M. and M.P.), furthermore by the Research Council for Biosciences and Environment of the Academy of Finland (#202403, L.K.). Many friends and colleagues assisted during field work on several expeditions or provided samples: G. Delgado Castro, Y. Fang, C. Fischer, E. García del Rey, A. Gebauer, S.A. Golovatch, M. Kaiser, B. Martens, A. Ostastshenko, W. Schawaller, Y.-H. Sun in Nepal, Kirghzia/ Kazachstan and China; A.A. Nazarenko and O. Valchuk in Far East Siberia; J. Broggi, J. Illera, K. Koivula, M. Starke, M. Steinbüchel and H.-H. Witt on the Canary islands. M. Dörr provided kind and helpful hard- and software support.

Appendix A. Supplementary data

Supplementary data associated with this article can be found, in the online version, at doi:10.1016/j.ympev.2007.03.006.

References

Aguirre, E., Pasini, G., 1985. The pliocene–pleistocene boundary. Episodes 8, 116–120.

Ancochea, E., Hernán, F., Cendrero, A., Cantagrel, J.M., Fuster, J.M., Ibarrola, E., Coello, J., 1994. Constructive and destructive episodes in the building of a young oceanic island, La Palma, Canary island, and genesis of the Caldera de Taburiente. J. Volcanol. Geotherm. Res. 60, 243–262.

Arbogast, B.S., Slowinski, J.B., 1998. Pleistocene speciation and the mitochondrial DNA clock. Science 282, Technical comments.

Arbogast, B.S., Edwards, S.V., Wakely, J., Beerli, P., Slowinski, J.B., 2002. Estimating divergence times from molecular data on phylogenetic and population timescales. Annu. Rev. Ecol. Sys. 33, 707–740.

Barker, F.K., Cibois, A., Schikler, P., Feinstein, J., Cracraft, J., 2004. Phylogeny and diversification of the largest avian radiation. Proc. Natl. Acad. Sci. USA 101, 11040–11045.

Bollmer, J.L., Whiteman, N.K., Cannon, M.D., Bednarz, J.C., de Vries, T., Parker, P.G., 2005. Population genetics of the Galápagos Hawk (*Buteo galapagoensis*): genetic monomorphism within isolated populations. The Auk 122, 1210–1224.

Bromham, L., Woolfit, M., 2004. Explosive radiations and the reliability of molecular clocks: island endemic radiations as a test case. Syst. Biol. 53, 758–766.

Brown, W., George, M., Wilson, A.C., 1979. Rapid evolution of animal mitochondrial DNA. Proc. Natl. Acad. Sci. USA 76, 1967–1971.

Cooper, A., Lalueza, F.C., Anderson, S., Rambaut, A., Austin, J., Ward, R., 2001. Complete mitochondrial genome sequences of two extinct moas clarify ratite evolution. Nature 409, 704–707.

Crochet, P.-A., Desmarais, E., 2000. Slow rate of evolution in the mitochondrial control region of gulls (Aves: Laridae). Mol. Biol. Evol 17, 1797–1806.

Dickinson, E.C., 2003. The Howard & Moore Complete Check List of the Birds of the World, third ed. Christopher Helm, London.

Fleischer, R.C., McIntosh, C.E., Tarr, C., 1998. Evolution on a volcanic conveyor belt: using phylogeographic reconstructions and K–Ar-based ages of the Hawaiian islands to estimate molecular evolutionary rates. Mol. Ecol. 7, 533–545.

Fleischer, R.C., Kirchman, J.J., Dumbacher, J.P., Bevier, L., Dove, C., Rotzel, N.C., Edwards, S.C., Lammertink, M., Miglia, K.J., Moore, W.S., 2006. Mid Pleistocene divergence of Cuban and North American ivory-billed woodpeckers. Biol. Lett. 2 (3), 466–469.

García-Moreno, J., 2004. Is there a universal mtDNA clock for birds?. J. Avian Biol. 35 465–468.

Gautier, F., Clauzon, G., Suc, J.P., Cravatte, J., Violanti, D., 1994. Age et durée de la crise de salinité messinienne. Comptes Rendus de l'Académie des Sciences de Paris 318 (2), 1103–1109.

Gill, F.B., Slikas, B., Sheldon, F.H., 2005. Phylogeny of titmice (Paridae): II. species relationships based on sequences of the mitochondrial cytochrome *b* gene. The Auk 122, 121–143.

Godoy, J.A., Negro, J.J., Hiraldo, F., Donazar, J.A., 2004. Phylogeography, genetic structure and diversity in the endangered bearded vulture (*Gypaetus barbatus*, L.) as revealed by mitochondrial DNA. Mol. Ecol. 13, 371–390.

Griswold, C.K., Baker, A.J., 2002. Time to the most recent common ancestor and divergence times of populations of common chaffinches (*Fringilla coelebs*) in Europe and North Africa: insights into pleistocene refugia and current levels of migration. Evolution 56, 143–153.

Guillou, H., Carracedo, J.C., Pérez Torrado, F., Rodríguez Badiola, E., 1996. K–Ar ages and magnetic stratigraphy of a hotspot-induced, fast grown oceanic island: El Hierro, Canary islands. J. Volcanol. Geotherm. Res. 73, 141–155.

Hall, T.A., 1999. Bioedit: a user-friendly biological sequence alignment editor and analysis program for windows 95/98/NT. Nucl. Acids Symp. Ser. 41, 95–98.

Harrap, S., Quinn, D., 1996. Tits Nuthatches & Treecreepers. Christopher Helm, London.

Hewitt, G.M., 2004. The structure of biodiversity—insights from molecular phylogeography. Front. Zool. 1, 4.

Ho, S.Y.W., Larson, G., 2006. Molecular clocks: when times are a—changing'. Trends Genet. 22, 79–83.

Irwin, D.E., Alström, P., Olsson, U., Benowitz-Fredericks, Z.M., 2001. Cryptic species in the genus *Phylloscopus* (old world leaf warblers). Ibis 143, 233–247.

Johnson, K.P., Seger, J., 2001. Elevated rates of non-synonymous substitutions in island birds. Mol. Biol. Evol. 18, 874–881.

Johnson, N.K., Cicero, K., 2004. New mitochondrial DNA data affirm the importance of Pleistocene speciation in North American birds. Evolution 58, 1122–1130.

Klicka, J., Zink, R.M., 1997. The importance of recent ice ages in speciation: a failed paradigm. Science 277, 1666–1669.

Krajewski, C., King, D.J., 1996. Molecular divergence and phylogeny: rates and patterns of cytochrome *b* evolution in cranes. Mol. Biol. Evol. 13, 21–30.

Krijgsman, W., Hilgen, F.J., Raffi, I., Sierro, F.J., Wilson, D.S., 1999. Chronology, causes and progression of the Messinian salinity crisis. Nature 400, 652–655.

Kryukov, A., Iwasa, M.A., Kakizawa, R., Suzuki, H., Pinsker, W., Haring, E., 2004. Synchronic east–west divergence in azure-winged magpies (*Cyanopica cyanus*) and magpies (*Pica pica*). J. Zool. Syst. & Evol. Res. 42, 342–351.

Kvist, L., Rytkönen, S., 2006. Characterization of a secondary contact zone of the great tit *Parus major* and the Japanese tit *P. minor* (Aves: Passeriformes) in far Eastern Siberia with DNA markers. Zootaxa 1325, 55–73.

Kvist, L., Ruokonen, M., Lumme, J., Orell, M., 1999. Different population structures in northern and southern populations of the European blue tit (*Parus caeruleus*). J. Evol. Biol. 12, 798–805.

Kvist, L., Martens, J., Ahola, A., Orell, M., 2001. Phylogeography of a Palaearctic sedentary passerine, the willow tit (*Parus montanus*). J. Evol. Biol. 14, 930–941.

Kvist, L., Martens, J., Nazarenko, A.A., Orell, M., 2003a. Paternal leakage of mitochondrial DNA in the great tit (*Parus major*). Mol. Biol. Evol. 20, 243–247.

Kvist, L., Martens, J., Orell, M., Higuchi, H., 2003b. Evolution and genetic structure of the great tit (*Parus major* complex). Proc. R. Soc. Lond. B 270, 1447–1454.

Kvist, L., Virii, K., Dias, P.C., Rytkönen, S., Orell, M., 2004. Glacial history and colonization of Europe by the European blue tit *Parus caeruleus*. J. Avian. Biol. 35, 352–359.

Kvist, L., Broggi, J., Illera, J.C., Koivula, K., 2005. Colonisation and diversification of the blue tits (*Parus caeruleus teneriffae*-group) in the Canary islands. Mol. Phyl. Evol. 34, 501–511.

Kvist, L., Arbabi, T., Päckert, M., Orell, M., Martens, J., 2007. Population differentiation in the marginal populations of the great tit (*Parus major*). Biol. J. Linn. Soc. 90, 201–210.

Lovette, I.J., Birmingham, E., 1999. Explosive speciation in the new world *Dendroica* warblers. Proc. R. Soc. Lond. 266, 1629–1636.

Lovette, I.J., 2004. Mitochondrial dating and mixed support for the 2% rule in birds. The Auk 121, 1–6.

Marincovich, L., Gladenkov, A.Y., 1999. Evidence for an early opening of the Bering Strait. Nature 14, 149.

Martens, J., Eck, S., Päckert, M., Sun, Y.-H., 1999. The Golden-spectacled warbler *Seicercus burkii*—a species swarm. Zool. Abh. Dresden 50, 282–327.

Martens, J., Tietze, D.-T., Eck, S., Veith, M., 2004. Radiation and species limits in the Asian Pallas's warbler complex (*Phylloscopus proregulus* s.l.). J. Ornithol. 145, 206–222.

Martens, J., Tietze, D.T., Sun, Y.H., 2006. Molecular phylogeny of *Parus* (*Periparus*), a Eurasian radiation of tits (Aves: Passeriformes: Paridae). Zool. Abh. Mus. Tierkd. Dresden 55, 103–120.

Nazarenko, A.A., 1988. Recent history of the east palearctic avifauna: transzonal interchange of the forest elements between south and north Asia since the last 35 000 years. Proc. Int. 100 DO-G meeting. Current Topics Avian Biol., 81–87.

Nunn, G.B., Stanley, S.E., 1998. Body size effects and rates of cytochrome *b* evolution in tube-nosed seabirds. Mol. Biol. Evol. 15, 1360–1371.

Nunn, G.B., Cooper, J., Jouventin, P., Robuktson, C.J.R., Robektson, G.G., 1996. Evolutionary relationships among extant albatrosses (Procellariiformes: Diomedeidae) established from complete cytochrome *b* gene sequences. The Auk 113, 784–801.

Olsson, U., Alström, P., Sundberg, P., 2004. Non-monophyly of the avian genus *Seicercus* (Aves, Sylviidae) revealed by mitochondrial DNA. Zool. Scripta 33, 501–510.

Olsson, U., Alström, P., Ericson, P.G.P., Sundberg, P., 2005. Non-monophyletic taxa and cryptic species—evidence from a molecular phylogeny of leaf warblers (*Phylloscopus*, Aves). Mol. Phyl. Evol. 36, 261–276.

Päckert, M., Martens, J., Sun, Y.-H., Veith, M., 2004. The radiation of the *Seicercus burkii* complex and its congeners— molecular genetics and bioacoustics. ODE 4, 341–364.

Päckert, M., Martens, J., Nazarenko, A.A., Valchuk, O., Petri, B., Eck, S., Veith, M., 2005. The great tit, *Parus major*, a misclassified ring species. Biol. J. Linn. Soc. 86, 153–174.

Päckert, M., Martens, J., Dietzen, C., Wink, M., Kvist, L., 2006. Radiation of goldcrests (*Regulus regulus*) on the Atlantic islands: evidence of a new taxon from the Canary islands. J. Avian. Biol. 37, 364–380.

Paxinos, E.E., James, H.F., Olson, S.L., Sorenson, M.D., Jackson, J., Fleischer, R.C., 2002. MtDNA from fossils reveals a radiation of Hawaiian geese recently derived from the Canada goose (*Branta canadensis*). Proc. Natl. Acad. Sci. USA 99, 1399–1404.

Pearce, J.M., 2006. Minding the gap: frequency of indels in mtDNA control region sequence data and influence on population genetic analyses. Mol. Ecol. 15, 333.

Pereira, S.L., Baker, A.J., 2006. A molecular timescale for galliform birds accounting for uncertainty in time estimates and heterogeneity of rates of DNA substitutions across lineages and sites. Mol. Phyl. Evol. 38, 499–509.

Pereira, S.L., Grau, E.T., Wajntal, A., 2004. Molecular architecture and rates of DNA substitutions of the mitochondrial control region of cracid birds. Genome 47, 535–545.

Press, W.H., Flannery, B.P., Teukolsky, S.A., Vetterling, W.T., 1992. Numerical Recipes in C, second ed. Cambridge University Press, New York.

Randi, E., 1996. A mitochondrial cytochrome *b* phylogeny of the *Alectoris* partridges. Mol. Phyl. Evol. 6, 214–227.

Ruokonen, M., Kvist, L., 2002. Structure and evolution of the avian mitochondrial control region. Mol. Phyl. Evol. 23, 422–432.

Saitou, N., Nei, M., 1987. The neighbor-joining method: a new method for reconstructing phylogenetic trees. Mol. Biol. Evol. 4, 406–425.

Salzburger, W., Martens, J., Sturmbauer, C., 2002a. Paraphyly of the blue tit (*Parus caeruleus*) suggested from cytochrome *b* sequences. Mol. Phyl. Evol 24, 19–25.

Salzburger, W., Martens, J., Sturmbauer, C., 2002b. Phylogeography of the Eurasian willow tit (*Parus montanus*) based on DNA sequences of the mitochondrial cytochrome *b*. Mol. Phyl. Evol. 24, 26–34.

Sanderson, M.J., 1997. A non-parametric approach to estimating divergence times in the absence of rate constancy. Mol. Biol. Evol 14, 1218–1231.

Sanderson, M.J., 2003. r8s: inferring absolute rates of molecular evolution and divergence times in the absence of a molecular clock. Bioinformatics 19, 301–302.

Sanderson, M.J., 2004. r8s, version 1.70. User's manual (December 2004). Available from: ⟨http://ginger.ucdavis.edu/r8s/r8s1.7.manual.pdf.

Schmidt, H.A., Strimmer, K., Vingron, M., von Haeseler, A. 2000. Tree-Puzzle, version 5.0.—München.

Shields, G.F., Wilson, A.C., 1987. Calibration of mitochondrial DNA evolution in geese. J. Mol. Evol. 24, 212b–217b.

Swofford, D.L. 2001. "Paup*: Phylogenetic Analysis using Parsimony (and Other Methods)", version 4.06b. Sinauer Associates, Sunderland/Massachusetts.

Veith, M., Kosuch, J., Vences, M., 2003. Climatic oscillations triggered post-Messinian speciation of western Palearctic brown frogs (Amphibia, Anura, Ranidae). Mol. Phyl. Evol. 26, 310–327.

Veith, M., Mayer, C., Boudiema, S., Barroso, D.D., Bogaerts, S., 2004. J. Biogeogr. 31, 159–171.

Warren, B.H., Bermingham, E., Bowie, R.C.K., Prys-Jones, R., Thébaud, C., 2003. Molecular phylogeography reveals island colonization history and diversification of western Indian Ocean sunbirds (*Nectarinia*: Nectariniidae). Mol. Phyl. Evol. 29, 67–85.

West, F.R.S., 1988. The record of the cold stage. Philos. Trans. R. Soc. London B 318, 505–522.

Zink, R.M., 2005. Natural selection on mitochondrial DNA in *Parus* and its relevance for phylogenetic studies. Proc. R. Soc. London B 272, 71–78.